ROYAL SOCIETY
OF CHEMISTRY

## PAPER

Check for updates

# Hydrodynamic and ultrasonic cavitation physically modifies the milk protein concentrates with improved functionality

Shreyas H. K.,[a] Preeti Adhikari,[a] Anas Ejaz Yasmeen Shaikh [ID] [b] and Shalini S. Arya [ID] *[a]

Hydrodynamic cavitation (HC) and ultrasonic (US) treatments were applied to modify milk protein concentrates (MPCs) and enhance their techno-functional properties. Treatments were conducted at 6 MPa for 0–30 min (HC) and 20 kHz at 200–600 W (US). Both cavitation techniques significantly improved emulsifying, foaming, and solubility characteristics of MPCs. The emulsifying activity increased by up to 110% at 600 W, while foaming capacity improved by over 200% at 6 MPa, following 20 min treatments. A marked increase in protein solubility (up to 99.6%) and reduction in particle size (from 4.82 μm in control to 0.94 μm for US-treated and 1.35 μm for HC-treated samples) indicated disaggregation and unfolding of protein aggregates. Spectroscopic analysis further confirmed alterations in the secondary structure, with reduced amide I intensity and slight band broadening, signifying partial unfolding and exposure of hydrophobic residues. These structural modifications directly correlated with improved surface activity, resulting in enhanced emulsifying and foaming behavior. SDS-PAGE analysis confirmed the absence of protein degradation, indicating that cavitation induced conformational rather than chemical changes. Overall, the findings substantiate that cavitation treatments effectively unfolded protein structures and exposed hydrophobic groups, leading to improved functional performance. This study highlights the potential of scalable cavitation processes for producing high-performance, clean-label dairy ingredients suitable for industrial food applications.

### Sustainability spotlight

Our work underscores the potential of advanced cavitation technologies like hydrodynamic and ultrasonic, in enhancing the functional properties of milk proteins without chemical additives. By improving solubility, emulsification, and foaming capacity, these non-thermal, energy-efficient methods contribute to sustainable food processing. This approach supports cleaner production practices, reduces reliance on synthetic additives, and aligns with circular economy principles. It advances the development of high-performance, protein-rich food products, supporting the United Nations' Sustainable Development Goals (SDGs), particularly Goal 9: industry, innovation, and infrastructure, and Goal 12: responsible consumption and production.

## 1 Introduction

Protein is crucial for maintaining overall health, muscle building, immune function, and enzyme activity.[1] It plays a significant role beyond nutrition, enhancing the texture, taste, and structure of food products.[2] Meat, dairy, grains, and legume proteins act as stabilizers, emulsifiers, thickeners, and gelling agents, making them indispensable in creating high-quality nutritious foods.[3] Dairy proteins like whey and casein are particularly noteworthy for their nutritional benefits. Whey is

quickly absorbed, while casein provides a sustained release of amino acids.[3] These proteins not only improve the texture, and flavor of products such as yogurt, cheese, and protein-enriched beverages[4–8] but also support muscle protein synthesis and weight management, making them popular among athletes and fitness enthusiasts.[2] A recent market survey highlights the increasing demand for dairy proteins driven by a growing focus on health and fitness.[7] This trend reflects consumer preferences for protein-enriched products, highlighting the importance of dairy proteins in modern diets and the evolving food industry landscape.

Native proteins are unstable under processing conditions (high temperature and extreme pH) and have poor solubility in water and other liquids, which limits their use in various food applications. Modification can improve stability, solubility, functional, and structural properties for diverse applications both in food and pharmaceuticals.[9–12]

[a]*Food Engineering and Technology Department, Institute of Chemical Technology, Mumbai, Maharashtra, 400019, India. E-mail: fbt22hk.shreyas@pg.ictmumbai.edu.in; adhikaripreeti97@gmail.com; ss.arya@ictmumbai.edu.in; Fax: +91-22-3361-1020; Tel: +91-22-3361-2511; +91-22-3361-1421*

[b]*Agricultural and Food Engineering Department, Indian Institute of Technology Kharagpur, Kharagpur, West Bengal, 721302, India. E-mail: anas.ehd.pmrf@gmail.com*

Traditional methods of modification, such as enzymatic and chemical, are two primary approaches extensively employed for this purpose. Enzymatic methods utilize specific enzymes to catalyze targeted reactions. On the other hand, chemical methods use various reagents to induce modifications, providing versatility and control over specific protein functionalities. Enzymatic hydrolysis of milk protein concentrates (MPCs) using a cocktail of protease enzymes such as trypsin, chymotrypsin, pepsin, and papain enzymes at various pH has shown to improve the solubility, emulsion activity, stability, foaming capacity, and emulsion capacity of casein and whey MPCs.[13] Enzymatic hydrolysis of proteins into smaller peptides also reduces the surface hydrophobicity and gel strength of MPCs and also increases solubility of milk protein isolate over a wide range of pH (4.0–7.0).[14] Likewise, chemical methods also improved the functional properties such as water binding capacity, emulsifying and foaming properties of MPCs.[15] However, both enzymatic and chemical methods come with challenges. Enzymatic modifications have limited scalability making them less suitable for large-scale industrial applications. However chemical methods often require stringent reaction conditions, potentially leading to undesired side reactions and alterations in protein bioactivity.[16] Furthermore, chemical reagents pose potential health risks, leaving traces of harmful residues in the product and affecting the final product quality as well.

In contrast, various green physical methods have emerged as promising alternatives for modifying proteins. Cold plasma treatment improves the wettability of MPCs and soy protein isolate by reducing the apparent contact angle of the powders caused due to hydrophilization.[17] High-pressure processing (HPP) has also shown to improve solubility and gelation ability of MPCs after treatment at 450 MPa for 15 min by weakening the non-covalent interactions between casein macromolecules.[15] Pulsed electric field (PEF) increases the gelation time of MPCs, but has no effect on other physicochemical properties.[18] These techniques bring several advantages, including reduced chemical usage, shorter processing times, and minimal impact on the nutritional quality of proteins, but the higher capital cost and industrial scalability pose significant challenges.[19]

HC and US are effective in protein modification and improving protein functionality without compromising its nutritional quality, which are challenging with traditional methods. Ultrasonic cavitation (US) disrupts proteins by breaking apart their non-covalent interactions, causing them to unfold, aggregate, and fragment into smaller peptides. It can also alter disulfide bonds, further denaturing and aggregating the proteins.[20] In contrast, HC generates powerful shear forces and micro-streaming effects that rearrange and distort the secondary structures of proteins. When bubbles collapse during HC, localized increases in temperature and pressure lead to protein denaturation and trigger chemical reactions like oxidation and hydrolysis, significantly impacting their secondary structure.[21] Both types of cavitation also affect the complex three-dimensional folding of proteins (tertiary structure) and enhance the physicochemical properties of proteins.[22] Careful control of cavitation parameters is essential to optimize

these effects while preserving protein functionality across various industrial applications.[23]

The potential for HC and US has been explored in soy protein isolates, which resulted in reduced surface hydrophobicity and improved solubility, thus improving the emulsifying and foaming properties of soy proteins.[22] A recent study by Patil and his colleagues demonstrated improvement in viscosity and alteration in the secondary structure of casein protein after HC treatment.[24] HC and US also showed a drastic reduction in microbial load and improvement in the physico-chemical properties of peanut milk.[25] Although there are numerous studies investigating the effect of ultrasonic cavitation on the physical and functional properties of MPCs, there is a need for investigating the dual effect of HC and US on functionality and physical properties of MPCs. This study provides a systematic, side-by-side comparison of hydrodynamic cavitation (HC) and probe ultrasonication (US) on milk protein concentrates under comparable energy conditions. Unlike earlier studies focusing on either technique individually, this work simultaneously evaluates physicochemical, functional, and structural changes to establish a direct comparison and identify the optimal cavitation route for industrial upscaling. In the current study, the effect of US and HC treatments on parameters like emulsifying properties, foaming properties, solubility, particle size, and protein structure has been explored.

## 2 Materials and methods

### 2.1. Materials

Milk protein (75–80%) was procured from Aseschem Chemicals, Jodhpur, India. All the chemicals used were of AR (Analytical Reagent) grade. Concentrated sulphuric acid, sodium hydroxide, hydrochloric acid, acetone, phenolphthalein, pH calibration buffers, alcohol, petroleum ether, sodium dodecyl sulphate kit, selenium, and anthrone were procured from Himedia Laboratory Private Ltd, Mumbai, India.

### 2.2. Methods

**2.2.1. Proximate analysis of MPCs.** Proximate composition was determined using the AOAC method (2002). In brief, moisture content was determined by drying samples in a hot air oven at 105 °C, fat extraction was performed using the Soxhlet method, and the Kjeldahl method was used to quantify proteins. A standard nitrogen-to-protein conversion factor of 6.38 for milk protein samples was used following the ISO 8968/IDF 20-1; 20-3 standard for total nitrogen determination in milk.[26] Ash content was assessed using a muffle furnace. Percentage carbohydrate was calculated by subtracting percentages of moisture, fat, protein, and ash from 100%. All the experiments were performed in triplicate.

**2.2.2. MPC solution preparation.** A 10% w/v MPC solution was prepared by dissolving 10.87 g of protein samples in 100 mL of distilled water, following the method outlined by Jokar and Azizi with slight modifications.[27] Homogenization was performed at 1300 rpm for 6 min to ensure the uniform dispersion and dissolution of milk protein in the aqueous medium. The

total soluble solids (TSS) of the solution were first estimated using a portable refractometer (°Brix scale) for a rapid indication of soluble content and was validated against a gravimetric test. Since refractive index also responds to dissolved proteins and salts, a calibration curve between refractometric and gravimetric TSS values was established to ensure accuracy. Both the methods showed similar results. Experiments were performed in triplicate.

**2.2.3. Modification of 10% w/v MPC using US.** The preparation of 10% w/v MPC involved ultrasonication as per the method outlined by Li *et al.* with minor adjustments, using a probe sonicator (Labman Probe 650).[22] The sonicator operated at a fixed frequency of 20 kHz and offered a range of power settings from 200 to 600 W, allowing for flexible intensity levels. Glass beakers housed the samples which underwent ultrasonication for durations of 5, 10, 20, and 30 min at 600 W with a pulse-on duration of 1 second and a pulse-off duration of 3 s. To maintain a consistent temperature throughout the process, a thermocouple was integrated into the experimental setup. Each sample had a volume of 100 mL and the temperature was kept below 50 °C to ensure optimal conditions for the ultrasonication procedure. Experiments were performed in triplicate.

**2.2.4. Modification of 10% w/v MPC using HC.** The HC of the MPC was performed following the method outlined by Li *et al.* with slight modifications.[22] The experimental setup used in this study was similar to that described by Pegu *et al.*[28] in their work on the application of different orifice configurations for hydrodynamic cavitation-induced inactivation of *Escherichia coli* and *Staphylococcus aureus* in milk. The setup included a holding tank, a centrifugal pump, control valves (V1 andV2), pressure gauges, and a venturi tube and required a minimum operational volume of 2.5 L. A 2.5 L solution containing 10% w/v MPC was introduced into the holding tank. Upon activating the centrifugal pump, the liquid circulated from the holding tank through the venturi tube, with pressure regulation controlled by valve V2. Cavitation treatment was carried out on the MPC at 6 MPa pressure for durations ranging from 5 to 30 min, maintaining a constant flow rate of 24 L min⁻¹ across various operational parameters. After treatment the sample solution was promptly stored at 4 °C to preserve their integrity. Experiments were done in triplicate.

**2.2.5. Effect of US & HC on the emulsifying properties in control and physically modified MPCs.** The emulsifying properties of both raw and modified protein samples were analyzed according to Li *et al.* with slight modifications.[22]

*2.2.5.1 Emulsifying activity.* In this experimental procedure, 10 mL of the previously prepared MPC solution was mixed with an equal volume of rice bran oil. The resulting emulsified mixture was then centrifuged at a speed of 1100 rpm for 10 min. After centrifugation, measurements were taken to determine the heights of the emulsified layer ($H_e$) and total mixture ($H_t$) in the tube. This method was employed to evaluate the emulsification characteristics and phase separation behavior of the protein solution in the presence of rice bran oil providing valuable insights into its emulsifying properties. The emulsifying activity (EA) was determined using eqn (1).

$$EA = \left(\frac{H_e}{H_t}\right) \times 100 \quad (1)$$

*2.2.5.2 Emulsifying stability.* Following the homogenization of the emulsion in the above emulsifying activity method, a further step was taken to heat the emulsified mixture to a temperature of 80 °C and this temperature was maintained for a duration of 30 min. Subsequently, the emulsified sample underwent centrifugation at 1100 rpm for 10 min. Subsequent calculations involved determining the emulsion stability (ES) expressed as percentage, which was computed using eqn (2). This calculation allowed for the quantitative evaluation of emulsion stability, based on the heights of the emulsified layer before ($H_{e,0}$) and after ($H_{e,t}$) the heating process. Measurements were done in triplicate.

$$EA = \left(\frac{H_{e,t}}{H_{e,0}}\right) \times 100 \quad (2)$$

**2.2.6. Effect of US & HC on the foaming properties in control and physically modified MPCs.** The foaming property analysis was done according to the method described by Li *et al.* with slight modifications.[22] In this experimental procedure, 30 mL of 10% w/v MPC was subjected to homogenization at a high rotational speed of 10 000 rpm for a duration of 1 min. Subsequently, two volume measurements were recorded, namely the initial volume immediately after homogenization ($V_0$) and the volume after allowing the sample to stand at room temperature for 6 min ($V_t$). In our preliminary experiments, the foam volume of the milk protein concentrate was observed to decay rapidly within the first 10 min, reaching equilibrium after approximately 6 min. Therefore, 6 min was selected as the time for comparing foaming stability across treatments. The determination was done in triplicate. To assess the foaming characteristics of the protein solution, two key calculations were performed. Firstly, the foaming capacity (%), representing the ability of the solution to form foam, was determined using eqn (3). Secondly, the foaming stability (%), which indicates the longevity of the foam, was computed using eqn (4).

$$Foaming\ capacity(\%) = \left(\frac{V_0}{30}\right) \times 100 \quad (3)$$

$$Foaming\ stability(\%) = \left(\frac{V_t}{V_0}\right) \times 100 \quad (4)$$

**2.2.7. Effect of US & HC on the particle size in control and physically modified MPCs.** The particle size analysis was conducted using a Malvern Mastersizer 3000+ instrument.[22] The refractive index of deionized water which served as the dispersing phase was 1.330 and that of protein particles was 1.47. Homogenization of 10% w/v MPC was employed to ensure uniform particle distribution. 3 mL of this homogenized MPC was taken into the injector port of the particle size analyzer. Particle size measurements were reported as volume mean diameter or De Brouckere diameter ($d_{4,3}$), calculated using eqn

(5), where $n_i$ represents the number of particles of diameter $d_i$. Determinations were performed in triplicate to ensure accuracy and reliability of the results.

$$d_{4,3} = \frac{\sum n_i d_i^4}{\sum n_i d_i^3} \qquad (5)$$

**2.2.8.   Effect of US & HC on the solubility in control and physically modified MPCs.** Protein solubility was determined as per the method outlined by Malik *et al.* with slight modifications.[20] Two identical samples of the 10% w/v protein concentrate were prepared. In the first sample, centrifugation at 3000 rpm for 15 min was carried out. The supernatant phase was carefully collected and placed into a clean container. The second sample, serving as control, was kept without centrifugation. Subsequently, both the supernatant and control samples were evenly distributed in separate plates and subjected to drying for 24 h at 60 °C. The drying process continued until three consecutive weight measurements indicated no further changes in the sample masses, signifying that the drying process had reached completion. These weight measurements, which represented the dry weights of the centrifuged and uncentrifuged samples, were then employed to determine the solubility of the protein. The solubility percentage was calculated using eqn (6), where $M_{d,test}$ and $M_{d,control}$ represent the dry weights of the supernatant from the centrifuged sample and the uncentrifuged (control) sample, respectively. In addition, the soluble protein fraction was quantified using Bradford colorimetric assay with bovine serum albumin (BSA) as the standard as described by Voudouris *et al.*[29] Briefly, 20 μL of appropriately diluted supernatant (1 : 10 dilution in phosphate buffer) was mixed with 180 μL of the Bradford reagent in a 96-well microplate and incubated for 10 min at room temperature. Absorbance was measured at 595 nm using a microplate reader. A BSA standard curve (0–200 μg mL$^{-1}$) was constructed, showing a linear relationship ($R^2 \approx 0.999$). The soluble protein concentration of each sample was calculated from the standard curve, corrected for dilution, and expressed as μg mL$^{-1}$. All samples were analyzed in triplicate.

$$\text{Solubility}(\%) = \left( \frac{M_{d,test}}{M_{d,control}} \right) \times 100 \qquad (6)$$

**2.2.9.   Effect of US & HC on the turbidity in control and physically modified MPCs.** To determine turbidity for the 10% w/v MPC sample, the experimental procedure involved placing the sample in a spectrophotometer to measure absorbance at a wavelength of 600 nm.[30] Prior to sample analysis, the spectrophotometer was calibrated, ensuring accurate and reliable absorbance measurements. Milli-Q water was employed as the blank for baseline correction during absorbance readings. The absorbance values obtained in this manner were utilized to assess turbidity in the milk protein concentrates quantitatively.

**2.2.10.   Effect of US & HC on the pH in control and physically modified MPCs.** The pH analysis was carried out with 100 mL of the 10% w/v MPC sample using a pH meter.[22] Before the analysis, the pH meter was appropriately calibrated using standard buffer solutions with known pH values, typically pH 7 and pH 10. Once the pH meter was calibrated, milk protein concentrates were analyzed using the calibrated pH meter to determine their pH values.

**2.2.11.   Effect of US & HC on the secondary structures in control and physically modified MPCs.** Fourier transform infrared (FTIR) analysis of milk protein concentrates was conducted using a JASCO-6600, a model of ATR (Attenuated Total Reflectance) FT-IR spectrometer manufactured by the JASCO company, following the methodology outlined by Kalkan *et al.* with slight modifications.[31] Prior to analysis, the samples were dried in a hot air oven at 50 °C for 24 h. This drying protocol effectively reduced the moisture content within the samples, thereby mitigating the disruptive influence of water in FTIR analysis. After the drying step, the dried milk protein samples were finely ground to ensure uniform distribution in the FTIR sample holder. FTIR spectral data were then collected using instrument settings tailored to the characteristics of the dried samples. Acetone was used to clean the injection port. The background subtraction was carried out using Origin Pro software to account for instrumental and environmental interferences. Data analysis was conducted to identify key spectral peaks. These procedures collectively facilitated the extraction of pertinent information from the FTIR spectra for further interpretation and analysis in the study of milk protein concentrates.

**2.2.12.   Effect of US & HC on the molecular integrity of control and physically modified MPCs determined using SDS-PAGE analysis.** The SDS-PAGE analysis was conducted using a Mini-Protean Tetra system equipped with a PowerPac basic power supply.[22] The gel system employed a 12% separating gel and a 5% stacking gel, following a discontinuous buffered system. Milk protein concentrate samples underwent preparation by mixing with sample buffer (composed of 62.5 mM Tris–HCl, 2% SDS, 25% glycerol, 0.01% bromophenol blue, and 5% 2-mercaptoethanol with pH 6.8) in a ratio of 1 : 2 (v/v). Subsequently, the mixed samples were heat-treated at 100 °C for 5 min, followed by cooling to room temperature before electrophoresis. For each lane 20 μL of the sample along with 10 μL of ladder was loaded onto the gel. Test protein or commercial bovine lactoferrin (Sigma-Aldrich) was included as a reference standard to facilitate identification of the major whey protein bands. Post-electrophoresis gel immobilization was carried out using an immobilization solution (comprising ethanol/acetic acid/deionized water in a ratio of 500/100/400 v/v/v). Staining of the gel was performed with a solution containing methyl alcohol/acetic acid/deionized water (in a ratio of 500/100/400 v/v/v) and 0.06% (w/v) Coomassie brilliant blue R-250. After staining, the gel was destained with a solution containing acetic acid, methyl alcohol, and deionized water in a ratio of 75 : 50 : 875 (v/v/v).

**2.2.13.   Statistical analysis.** All experiments were carried out in triplicate, and the results are presented as mean ± standard deviation. The data were subjected to one-way analysis of variance (ANOVA) using SPSS 12.0 software (SPSS Inc., Chicago, IL, USA) to determine whether significant differences existed among treatment means. When the ANOVA indicated

significance ($p < 0.05$), Tukey's multiple-comparison test was applied to identify which means differed significantly.

# 3 Results and discussion

## 3.1. Proximate composition of MPCs

The results of proximate composition are shown in Table 1. The moisture content of the sample was 4.16 ± 0.03% with 3.53 ± 0.05% fat, whereas the protein content recorded was 80 ± 0.11%. The dominance of protein in the sample signifies a significant proteinaceous nature possibly indicating a concentrated protein source which is similar to previous experiments.[32,33] The ash content reflects the mineral composition, and the carbohydrate proportion aligns with the non-proteinaceous and non-fat components (Table 1).

## 3.2. Effect of US on the emulsifying and foaming properties in control and physically modified MPCs

Based on the lack of significant changes observed in emulsifying and foaming properties within the 300 to 500 W power range and guidance from the review paper the decision was made to increase the sonication power to 600 W.[34] This adjustment was intended to provide the necessary energy input for more substantial protein modifications, with the potential to enhance emulsifying and foaming properties. Emulsifying

activity (EA) is the capacity of proteins to integrate in a water and oil interconnection, whereas emulsifying stability (ES) is a measure of tolerance of the emulsion post-storage and heat treatment. Foaming activity and stability are two pivotal properties of proteins and depend on their ability to unfold and adsorb at the air–water interface to stabilize air bubbles. Table 2 shows the impact of US on EA and ES on milk protein concentrates with changes in treatment duration.

**3.2.1. Emulsifying activity.** Table 2 summarizes the effect of US on the emulsifying properties of 10% w/v MPC at different pressures and treatment times. After being subjected to US treatment at a range of 200 to 600 W, a significant increase in EA was observed in comparison with the control. At 200 W, the EA slightly decreased to 41.35%, which was not statistically different from the control ($p > 0.05$). However, increases of 42.1% and 43.72% were observed at 10 and 20 min, respectively. These findings were similar to the results reported in the previous studies.[35]

With treatment at 300 W for 20 min, 400 W for 10 min, and 500 W for 20 min, a significant increase in EA was observed in comparison to the control. These observations were consistent with the findings of Zhang et al.[36] However, at 600 W for 20 min, a 110% change in the emulsifying activity was observed as compared to the control (Table S1). As seen in Fig. S1, the EA at 600 W increased to 54.93%, 75.06%, and 91.46% with 5, 10 and 20 min of treatment, respectively, a significant increase compared to the control ($p < 0.05$). This increase was attributed to the high energy generated by ultrasonic waves, which can partially unfold protein molecules, exposing hydrophobic groups that were previously buried within the protein structure.[37] As seen in Table 2, prolonged exposure to ultrasound for 30 min resulted in a high emulsifying activity of 86.1%, significantly different from the control ($p < 0.05$) but less than the previous result at 20 min. This indicates that continued unfolding of protein structures contributes to enhanced functionality.[37]

**Table 1** Proximate composition of MPCs[a]

| Parameter | Composition (%) |
|---|---|
| Moisture | 4.16 ± 0.03 |
| Fat | 3.53 ± 0.05 |
| Protein | 80.86 ± 0.11 |
| Ash | 2.16 ± 0.05 |
| Carbohydrate | 10.85 ± 0.25 |

[a] Results are expressed as mean ± standard deviation.

**Table 2** Effect of ultrasonic cavitation at 20 kHz subjected to different ultrasound power and treatment times on the emulsifying and foaming properties of 10% w/v MPC[a]

| Processing condition | Ultrasound power (W) | Treatment time (min) | Emulsifying activity (%) | Emulsifying stability (%) | Foaming activity (%) | Foaming stability (%) |
|---|---|---|---|---|---|---|
| Control | 0 | 0 | 42 ± 0.50[fg] | 47.06 ± 0.20[bc] | 19.7 ± 0.26[f] | 41.2 ± 0.17[b] |
| 1 | 200 | 5 | 41.35 ± 0.34[g] | 46.21 ± 0.55[c] | 20.83 ± 0.41[ef] | 40.55 ± 0.78[b] |
| 2 | 200 | 10 | 42.10 ± 0.17[fg] | 46.91 ± 0.45[bc] | 21.54 ± 0.55[ef] | 42.55 ± 0.24[ab] |
| 3 | 200 | 20 | 43.72 ± 0.25[fg] | 47.33 ± 0.28[bc] | 21.93 ± 0.30[ef] | 42.16 ± 0.28[ab] |
| 4 | 300 | 5 | 44.78 ± 0.78[fg] | 47.98 ± 0.77[bc] | 22.55 ± 0.45[ef] | 42.54 ± 0.19[ab] |
| 5 | 300 | 10 | 46.53 ± 0.50[f] | 48.92 ± 0.17[bc] | 22.43 ± 0.51[ef] | 43.33 ± 0.57[ab] |
| 6 | 300 | 20 | 48.43 ± 0.51[ef] | 49.02 ± 0.13[bc] | 23.52 ± 0.52[e] | 43.86 ± 0.11[ab] |
| 7 | 400 | 5 | 48.65 ± 0.48[ef] | 49.88 ± 0.25[bc] | 23.54 ± 0.48[e] | 43.88 ± 0.55[ab] |
| 8 | 400 | 10 | 49.44 ± 0.50[e] | 50.72 ± 0.36[b] | 24.32 ± 0.42[de] | 44.43 ± 0.51[ab] |
| 9 | 400 | 20 | 49.39 ± 0.57[e] | 50.82 ± 0.15[b] | 25.6 ± 0.52[de] | 44.56 ± 0.45[ab] |
| 10 | 500 | 5 | 50.12 ± 0.78[de] | 51.25 ± 0.44[b] | 26.88 ± 0.65[de] | 45.55 ± 0.58[ab] |
| 11 | 500 | 10 | 50.88 ± 0.09[de] | 52.11 ± 0.17[ab] | 26.76 ± 0.25[de] | 46.66 ± 0.41[a] |
| 12 | 500 | 20 | 51.61 ± 0.53[de] | 52.6 ± 0.76[ab] | 27.83 ± 0.16[de] | 46.9 ± 0.17[a`] |

[a] Results are expressed as mean ± standard deviation. Different lowercase letters indicate significant differences in each column for each treatment ($p < 0.05$).

**3.2.2. Emulsifying stability.** On comparing with the control, it can be seen that the US treatment at 200 W for 5 min and 10 min decreased ES slightly to 46.21% and 46.9%, respectively, which were not statistically different from the control ($p > 0.05$). The observed effects can be attributed to differences in energy input among the high-intensity ultrasound treatments at varying power levels, where higher power facilitated greater cavitational effects and protein modification. As a result, the energy transferred to the milk proteins may be insufficient to disrupt strong hydrophobic interactions adequately, which are crucial for stabilizing emulsions by allowing proteins to adsorb at the oil–water interface and form a protective layer.[38]

Extending the treatment time further to 20 min under the same power conditions led to an ES of 47.33%, which can be seen in Table 2. Although slightly higher than the previous treatments, it was also not statistically significant compared to the control sample. These findings are consistent with the study by Li *et al.*[38] A significant increase in ES was noted for treatments at 300, 400, and 500 W in comparison with the control. These results are consistent with the findings of Zhang *et al.*[36] However, the best result was achieved at 600 W for 20 min (54.2%), which was significantly higher than the control ($p < 0.05$). Fig. S2 demonstrates ES at variable times ranging from 0 to 30 min at 600 W.

These observed effects suggest that high-intensity ultrasound cavitation can effectively disrupt non-covalent interactions between protein molecules, such as hydrogen bonds and van der Waals forces. This disruption leads to a more flexible protein network that is better able to stabilize emulsions by forming a viscoelastic interfacial layer and exposing more hydrophobic residues.[39] After 30 min of sonication, the stability was 56.2%, which was statistically different from the control ($p < 0.05$), suggesting that prolonged ultrasound exposure enhances the formation of stable emulsions by promoting protein rearrangement and stronger interfacial interactions.

**3.2.3. Foaming activity.** As seen in Table 2, an increase in foaming activity (FA) as compared to the control was noted as exposure power increased from 200 to 500 W. A significant increase in FA was noted at 20 min across all power treatments (200, 300, 400, and 500 W) compared to the control, similar to the findings by Jambrak *et al.*[40] On increasing the power to 600 W, for 20 min, a 200% change in the FA was observed as compared to the control as shown in Table S1. The FA at 600 W increased to 28%, 35.5%, and 86.53% with 5, 10, and 20 min of treatment, respectively, a significant increase from the control ($p < 0.05$) (Fig. S3).

This enhancement is attributed to the ultrasonic treatment partially unfolding protein molecules and exposing hydrophobic groups that facilitate interactions at the air–water interface. This unfolding is essential for stabilizing the air bubbles in foam.[41] After 30 min of sonication, foaming activity substantially increased to 112.53%, which was statistically different from the control ($p < 0.05$). These results suggest that extended sonication can promote protein rearrangement and stronger interfacial interactions, as lower ultrasound power

settings within the high-intensity range may not provide sufficient cavitational energy to induce extensive protein unfolding or structural modification.[42]

**3.2.4. Foaming stability.** The control sample exhibited a baseline foaming stability (FS) of 41.2%, similar to the findings by Alarcon-Rojo *et al.*[43] From Table 2, it can be observed that at lower power levels, ultrasound may not induce sufficient denaturation or rearrangement of protein structures critical for enhancing foaming stability, as FS for 5 and 10 min didn't show a significant difference from the control ($p > 0.05$). However, upon extending the treatment duration to 20 min at 300, 400, and 500 W, there was a significant increase in FS with respect to the control. These findings align with the research done by Zhang *et al.*,[36] indicating that intermediate ultrasound intensities can alter protein conformations in ways that compromise intermolecular interactions needed for stable foams. It is known that intermediate ultrasound power levels (300–500 W) can induce partial unfolding of proteins, potentially exposing hydrophobic residues that aid in interfacial interactions required for stable foams.[44]

However, at 600 W, FS demonstrated a significant reduction with increasing sonication duration. After 5 min, stability decreased markedly to 32.73%, which was less than the control. As seen in Fig. S4, this value further decreased to 30.66%, 24.66%, and 19.93% at 10, 20 and 30 min of sonication, respectively. Intense ultrasound at 600 W can induce extensive unfolding of protein molecules, exposing more hydrophobic residues that facilitate stronger protein–protein interactions at the air–water interface, thereby decreasing foaming stability.[40] These findings are indicative of the effects of possible protein reorganization or the impact of overprocessing on foaming stability.

## 3.3. Effect of HC on the emulsifying and foaming properties in control and physically modified MPCs

Based on the lack of significant changes observed in emulsifying and foaming properties within the pressure range of 1 to 5 MPa and guidance from the literature review, it was decided to increase the HC power to 6 MPa.[45] This adjustment was intended to provide the necessary energy input for more substantial protein modifications, with the potential to enhance emulsifying and foaming properties. Table 3 shows the impact of varying pressure (2.5–7 MPa) and treatment time (5–30 min) on the physical properties of milk protein concentrates.

**3.3.1. Emulsifying activity.** From Table 3, it is seen that the control sample, which underwent no HC treatment, showed an emulsifying capacity of 42%, aligning with the findings of Li *et al.*[22,23] Although, HC treatment at 2.5 MPa for 5 min was not statistically different from the control ($p > 0.05$). EA increased gradually with increasing treatment time and pressure. At 2.5 MPa for 30 min, EA was found to be 47%. As the pressure further increased to 5 MPa, a consistent increase in emulsifying capacity was observed. The highest activity was noted for 30 min (49.5%), which was significantly different from that of the control ($p < 0.05$). However, at 6 MPa for 20 min, a 112% change

**Table 3** Effect of hydrodynamic cavitation subjected to different pressures and treatment times on the emulsifying and foaming properties of 10% w/v MPC[a]

| Processing condition | Pressure (MPa) | Treatment time (min) | Emulsifying capacity (%) | Emulsifying stability (%) | Foaming capacity (%) | Foaming stability (%) |
|---|---|---|---|---|---|---|
| Control | 0 | 0 | 42.02 ± 0.51[ef] | 47.06 ± 0.20[bc] | 19.71 ± 0.26[f] | 41.20 ± 0.17[b] |
| 1 | 2.5 | 5 | 42.83 ± 0.76[ef] | 48.66 ± 0.57[c] | 24.33 ± 0.57[bc] | 41.16 ± 0.76[b] |
| 2 | 2.5 | 10 | 42.51 ± 0.86[ef] | 50.01 ± 1.02[ba] | 25.66 ± 0.57[b] | 43.66 ± 0.57[ab] |
| 3 | 2.5 | 20 | 44.03 ± 0.53[e] | 49.33 ± 0.57[bc] | 26.83 ± 0.76[e] | 43.51 ± 0.50[ab] |
| 4 | 2.5 | 30 | 47.04 ± 0.50[de] | 49.83 ± 1.04[bc] | 26.66 ± 1.15[e] | 43.66 ± 0.57[ab] |
| 5 | 5 | 5 | 46.8 ± 10[de] | 50.33 ± 1.15[bc] | 27.66 ± 0.57[ef] | 44.83 ± 0.76[ab] |
| 6 | 5 | 10 | 47.33 ± 0.57[de] | 50.33 ± 0.57[bc] | 27.50 ± 05[ef] | 45.83 ± 0.76[a] |
| 7 | 5 | 20 | 48.33 ± 1.15[d] | 52.5 ± 0.86[bc] | 27.66 ± 1.15[ef] | 45.89 ± 1.04[a] |
| 8 | 5 | 30 | 49.51 ± 0.50[d] | 52.66 ± 1.52[bc] | 28.66 ± 0.57[de] | 46.02 ± 1.01[a] |
| 13 | 7 | 5 | 44.33 ± 0.57[e] | 50.83 ± 0.76[bc] | 31.33 ± 0.28[d] | 38.25 ± 0.22[bc] |
| 14 | 7 | 10 | 44.01 ± 1.02[e] | 49.16 ± 1.05[bc] | 29.33 ± 1.15[de] | 38.66 ± 1.15[bc] |
| 15 | 7 | 20 | 43.16 ± 1.00[ef] | 48.50 ± 0.86[c] | 29.16 ± 0.28[de] | 38.83 ± 0.76[bc] |
| 16 | 7 | 30 | 42.33 ± 1.15[a] | 47.83 ± 0.76[c] | 27.05 ± 1.14[de] | 38.16 ± 1.15[bc] |

[a] Results are expressed as mean ± standard deviation. Different lowercase letters indicate significant differences in each column for each treatment ($p < 0.05$).

in emulsifying activity was observed as compared to the control (Table S2). Fig. S5 shows FS of the MPC with HC treatment at 6 MPa in a varying time range from 0 to 30 min. The peak activity at 20 min could be due to optimal unfolding and adsorption at the oil–water interface.[46,47] The subsequent decline at 30 min might be due to protein denaturation and aggregation, which reduce emulsifying efficiency.

Finally, at 7 MPa, the EA showed mixed results. EA decreased to 44.33% after 5 min treatment and further reduced to 42.33% at 30 min, which was not statistically different from the control ($p > 0.05$). These results indicate that the energy provided by higher cavitation pressures might not always result in effective emulsification, as prolonged exposure could lead to excessive protein aggregation and reduced surface activity, aligning with the findings of Anandharamakrishnan.[48]

**3.3.2. Emulsifying stability.** From Table 3, it can be seen that the control sample, which underwent no HC treatment, showed an emulsifying stability of 47.06%. When subjected to HC treatment at 2.5 MPa, the ES was highest at 10 min of treatment (50%), which, although higher than the control, was not statistically significant compared to it. These findings aligned with the results reported by Hou et al.[49] This pressure was insufficient to unfold the complex tertiary structures of milk proteins and expose the buried hydrophobic residues necessary for effective ES. As pressure further increased to 5 MPa, a consistent increase in emulsifying stability was observed. Prolonging the treatment to 20 min and 30 min at 5 MPa resulted in significantly increased ES as compared to that of the control ($p < 0.05$). A similar pattern was reported in a previous study, indicating that moderate cavitation pressure might start to partially unfold protein molecules, exposing some hydrophobic residues.[50]

At a pressure of 6 MPa, a more pronounced increase in emulsifying stability was observed, which was a significant improvement compared to the control ($p < 0.05$). The highest ES was achieved at 30 min of treatment (Fig. S6). The peak stability

at 20 min could be due to optimal unfolding and adsorption at the oil–water interface.[46,47] The subsequent plateau at 30 min might be due to the stabilization of the emulsion and optimal coverage of the oil–water interface by the unfolded proteins. However, the ES declined as there was further increase in pressure (Table 3).

**3.3.3. Foaming activity.** The untreated sample showed a foaming activity (FA) of 19.7%, which increased with HC treatment at 2.5, 5, and 6 MPa at varying durations (Table 3). At 2.5 and 5 MPa, the FA increased to 26.66% and 28.66%, respectively, which was not statistically different from the control ($p > 0.05$). These results align with the findings of Hou et al.,[49] suggesting that low HC pressures may not induce significant denaturation of milk proteins, which is necessary to enhance their surface activity. HC at this pressure might not produce enough shear forces to effectively disrupt the tertiary and quaternary structures of the proteins, thus failing to expose the hydrophobic residues necessary for improved air–water interfacial adsorption.[51]

At 6 MPa, there was a significant improvement with a 250% change in FA as compared to that of the control (Table S2). This significant increase in foaming capacity at higher pressure is likely due to more intense cavitation effects, which lead to greater protein unfolding and exposure of hydrophobic residues. These exposed hydrophobic groups improve the proteins' ability to stabilize air bubbles by forming more cohesive and elastic films at the air–water interface. After 20 min of treatment, foaming capacity reached its peak at 93.83%, a substantial improvement compared to the control ($p < 0.05$) (Fig. S7).[52] The peak foaming capacity at this stage suggests optimal protein modification, where the balance between unfolding and aggregation maximizes the surface activity of the proteins. However, extending the treatment to 30 min resulted in a decrease in FA, although still significantly higher than the control ($p < 0.05$). Like emulsion stability, prolonged HC treatment reduced the FA (Table 3). Prolonged cavitation may lead to overprocessing, causing further

unfolding, partial degradation, or excessive aggregation of protein molecules, negatively impacting foaming capacity.[23] Overprocessing can lead to the formation of larger aggregates, which are less effective at forming stable foam as they cannot uniformly cover the air bubbles.[53]

**3.3.4. Foaming stability.** The control sample exhibited a baseline foaming stability (FS) of 41.2%. HC treatments at 2.5 MPa for 5, 10, 20, and 30 min were not statistically significant ($p > 0.05$) to that of the control. These findings echoed the results reported by Hou et al.,[51] suggesting that the pressure and energy provided by low HC are insufficient to effectively unwind and expose the hydrophobic residues of the proteins. At 5 MPa, foaming stability improved substantially over treatment durations of 5 to 30 min, all statistically different from the control ($p < 0.05$) (Table 3). These observations align with the findings of Jambrak et al.,[40] suggesting that the intense shear forces generated by HC reduce the size of protein aggregates. Smaller particles have a larger surface area to volume ratio, which enhances their ability to adsorb at the air–water interface, promoting foam formation. Additionally, cavitation causes partial unfolding of protein molecules, exposing hydrophobic groups that facilitate interactions at the air–water interface. This improves the proteins' ability to stabilize air bubbles, increasing foaming stability.[37]

At 6 MPa (Fig. S8) and 7 MPa, the foaming stability decreased compared to the previous trials, all statistically different from the control ($p < 0.05$). These variations suggest that while moderate increases in pressure may influence foaming stability, the overall effect is influenced by other factors under the experimental conditions. Prolonged cavitation (beyond 20 min) can lead to overprocessing, where excessive mechanical stress causes further unfolding, partial degradation, or excessive aggregation of protein molecules.[48] These changes can negatively impact the proteins' ability to stabilize foam. Extended cavitation may induce the formation of larger protein aggregates through protein–protein interactions. Larger aggregates are less effective at forming a cohesive film around air bubbles, reducing foaming stability.[51]

### 3.4. Effect of US & HC on the particle size in control and physically modified MPCs

The effect of US and HC on the particle size in control and physically modified milk protein concentrates is shown in Fig. 1. It was observed that the control sample with no ultrasound treatment had a particle diameter of 4.82 ± 0.02 μm. For the sample sonicated for 5 min at 600 W (trial T1), the particle diameter decreased to 3.84 ± 0.03 μm, which was statistically different from the control ($p < 0.05$). This size reduction can be attributed to the disruptive effects of ultrasound on the protein's structural integrity as ultrasonic waves generate cavitation bubbles, which collapse and generate intense localized shear forces and shockwaves. These mechanical forces act upon the protein structure, leading to the disintegration of larger aggregates or particles into smaller entities.[22]

In subsequent trials (T2, T3, and T4), as the sonication time increased, further reductions in the particle size were
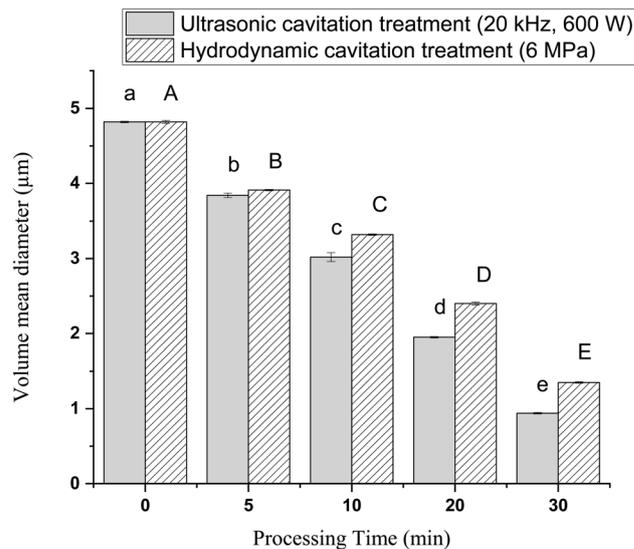


Fig. 1 Particle size expressed as volume mean diameter ($d_{4.3}$) of 10% w/v MPC modified using ultrasonic cavitation and hydrodynamic cavitation treatments for various time intervals (5, 10, 20, and 30 min) compared to the control sample (untreated). Different lowercase letters at the top of the bars indicate significant differences ($p < 0.05$) in each bar among samples treated at different times.

observed.[54] In T2 (10 min), the diameter decreased to 3.02 ± 0.06 μm, which was statistically different from both the control and T1 ($p < 0.05$). As reported earlier, prolonged US exposure continues to break down the protein's native structure and reduce the particle size by the formation of micro bubbles and an increased surface area, thereby enhancing the accessibility of the protein molecules to the disruptive forces.[20,55] In T3 (20 min) and T4 (30 min), the particle diameters further decreased to 1.95 ± 0.01 μm and 0.94 ± 0.01 μm, respectively, which were statistically different from all previous trials ($p < 0.05$).

With respect to HC, as seen in Fig. 1, the control sample, subjected to no pressure and 0 min of treatment, had a particle diameter of 4.82 ± 0.02 μm. However, with HC treatment in subsequent trials, significant reductions in the particle size were observed. In Trial 1 (T1), with 6 MPa pressure for 5 min, the particle diameter decreased to 3.91 ± 0.01 μm, which was statistically different from that of the control ($p < 0.05$). This reduction can be attributed to the unfolding or breaking of secondary protein structures due to the rupture of respective bonds like hydrogen, covalent and ionic bonds under the influence of HC.[56] As treatment time increases in subsequent trials to 10, 20 and 30 min (T2, T3, and T4, respectively), the particle size further reduced to 3.32 ± 0.01, 2.4 ± 0.02, and 1.35 ± 0.01 μm, respectively. This progressive reduction in the particle size can be attributed to the prolonged exposure to HC, where shear force and turbulence lead to the disruption of protein aggregates and the breakdown of protein structures.[22] The reduction in particle size indicates breakdown of larger protein aggregates into smaller particles, which can be attributed to the unfolding and disruption of protein structures induced by HC.[56] This phenomenon underscores the impact of

processing conditions, particularly time and pressure, on the physical characteristics of milk proteins under US & HC. Additionally, it aligns with the understanding that HC can induce structural changes in proteins, leading to alterations in their particle size and other physicochemical properties.

Both US and HC showed a similar progressive reduction in the particle size with increased cavitation time. However, the inter-treatment comparison indicates that US was more effective in reducing the particle size, where greater particle size reduction of 0.94 μm at 30 min was observed for US and slightly lower reduction of 1.35 μm at 30 min for HC. This can be attributed to the higher mechanical stress exerted by the localized ultrasonic shockwaves.[22]

### 3.5. Effect of US & HC on the solubility in control and physically modified MPCs

Protein solubility was evaluated using two complementary analytical methods: the gravimetric method, which represents total solids solubility, and the Bradford method, which quantifies the soluble protein fraction. This dual approach provided a comprehensive understanding of how ultrasound (US) and hydrodynamic cavitation (HC) treatments influenced both overall solid dispersion and protein-specific solubility.

As shown in Fig. 2a, Tables 4 and 5, solubility, expressed as a percentage, was strongly affected by processing conditions such as ultrasound power, cavitation intensity, and treatment time. In the gravimetric method, which measures total solubility, the control sample (untreated) exhibited a solubility of 94.2 ± 0.17%, while the solubilities of both US- and HC-treated samples were significantly ($p < 0.05$) higher than that of the control. In Trial 1 (T1), corresponding to 5 min of sonication at 600 W, the solubility increased to 95.5 ± 0.5%. As sonication time increased in subsequent trials (T2, T3, and T4), further improvements in solubility were observed, consistent with the findings of Kamal *et al.*,[57] indicating that the maximum disruptive effects of ultrasound treatment on the protein structure and enhanced solubility.

Similarly, in the Bradford method, which specifically quantifies the soluble protein content, the control sample showed a lower baseline solubility of 88.2 ± 0.17%, as this assay measures only the protein fraction. The solubilities of US- and HC-treated samples were significantly ($p < 0.05$) higher than the control, showing a similar enhancement trend as in the gravimetric results. In the case of ultrasonic cavitation (Table 4), solubility progressively increased with treatment time from 90.5 ± 0.51% (T1, 5 min) to 99.6 ± 0.17% (T4, 30 min). These results confirm that longer sonication durations led to greater unfolding and dispersion of proteins, supporting the conclusion that ultrasound-induced cavitation promotes structural disruption and improves solubility, in agreement with Kamal *et al.*[57]

The improvement in solubility observed by both methods can be attributed to the reduction in the particle size and disruption of protein aggregates caused by ultrasonic cavitation. Smaller protein particles have a higher surface area-to-volume ratio, facilitating enhanced interaction with the
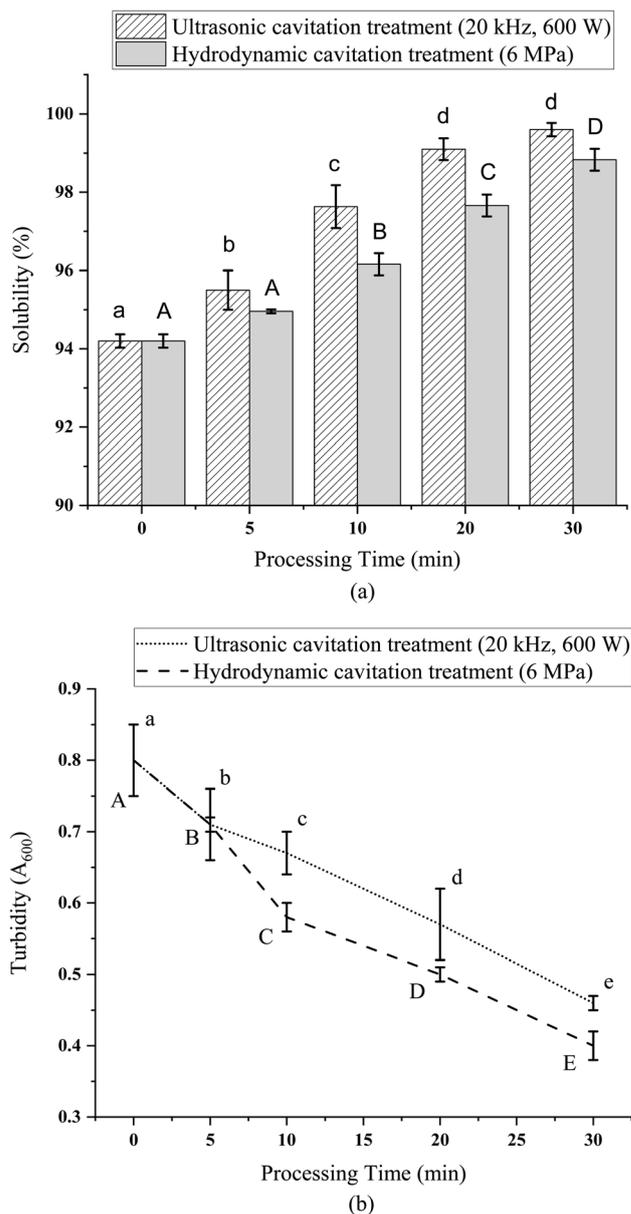


Fig. 2 (a) Solubility of 10% w/v MPC modified using ultrasonic cavitation and hydrodynamic cavitation treatments for various time intervals (5, 10, 20, and 30 min) compared to the control sample (untreated). (b) Turbidity evaluation of 10% w/v MPC modified using ultrasonic cavitation and hydrodynamic cavitation treatments for various time intervals (5, 10, 20, and 30 min) compared to the control sample (untreated). Different lowercase letters at the top of the bars indicate significant differences ($p < 0.05$) in each bar among samples treated at different times.

solvent. The cavitational forces generated during ultrasound treatment break down larger protein assemblies into finely dispersed particles that readily dissolve in the medium, as also described by Hou *et al.*[51]

For hydrodynamic cavitation (HC), both the gravimetric and Bradford results showed a consistent, time-dependent increase in solubility. In the gravimetric measurement, the total solubility increased steadily with treatment duration, while the

**Table 4** Effect of ultrasonic cavitation (20 kHz, 600 W) for 0–30 min on the solubility of 10% w/v MPC determined by the Bradford method. Here, control, T1, T2, T3, T4 represents 0, 5, 10, 20 and 30 min of ultrasonic cavitation processing time, respectively[a]

| Sample | Power (W) | Time (min) | Abs595 (mean ± SD) | Soluble protein (µg mL$^{-1}$) | Solubility (%) |
|---|---|---|---|---|---|
| Control | 0 | 0 | 0.18 ± 0.00 | 352.8 | 88.2 ± 0.17 |
| T1 | 600 | 5 | 0.19 ± 0.00 | 362.0 | 90.5 ± 0.51[a] |
| T2 | 600 | 10 | 0.19 ± 0.00 | 374.4 | 93.6 ± 0.55[b] |
| T3 | 600 | 20 | 0.20 ± 0.00 | 384.4 | 96.1 ± 0.28[c] |
| T4 | 600 | 30 | 0.21 ± 0.00 | 398.4 | 99.6 ± 0.17[d] |

[a] Results are expressed as mean ± standard deviation. Different lowercase letters indicate significant differences in each column for each treatment ($p < 0.05$).

**Table 5** Effect of hydrodynamic cavitation (6 MPa) for 0–30 min on the solubility of 10% w/v MPC determined by the Bradford method. Here, control, T1, T2, T3, T4 represents 0, 5, 10, 20 and 30 min of hydrodynamic cavitation processing time respectively[a]

| Sample | Pressure (MPa) | Time (min) | Abs595 (mean ± SD) | Soluble (µg mL$^{-1}$) | Solubility (%) |
|---|---|---|---|---|---|
| Control | 0 | 0 | 0.18 ± 0.00 | 352.8 ± 0.68 | 88.20 ± 0.17 |
| T1 | 6 | 5 | 0.19 ± 0.00 | 359.6 ± 0.20 | 89.90 ± 0.05[a] |
| T2 | 6 | 10 | 0.19 ± 0.00 | 372.4 ± 1.12 | 93.10 ± 0.28[b] |
| T3 | 6 | 20 | 0.20 ± 0.00 | 382.6 ± 1.12 | 95.66 ± 0.28[c] |
| T4 | 6 | 30 | 0.20 ± 0.00 | 395.3 ± 1.12 | 98.83 ± 0.28[d] |

[a] Results are expressed as mean ± standard deviation. Different lowercase letters indicate significant differences in each column for each treatment ($p < 0.05$).

protein solubility (Bradford assay, Table 5) increased from 88.2 ± 0.17% (control) to 98.8 ± 0.28% (T4, 30 min). At shorter durations (5 min, 6 MPa), the solubility increases to 89.9 ± 0.05%, which was not statistically significant ($p > 0.05$), suggesting limited structural modification during brief exposure. However, with longer processing times (10–30 min; T2–T4), solubility increased sharply to 93.1–98.8%, confirming that extended cavitation enhances solubilization. Similar findings were reported by Hou et al.,[51] who demonstrated that HC treatment of soybean glycinin (550 W, up to 20 min) increased surface hydrophobicity, reduced α-helix content, and increased β-sheet formation, all contributing to improved solubility.

The enhanced solubility observed under HC treatment can be explained by the intense shear forces and microturbulence generated during cavitation, which facilitate the dispersion and dissolution of protein aggregates. As processing time increases, these forces act continuously on protein molecules, breaking down larger structures into smaller and more soluble fragments. Additionally, cavitation-induced shear forces promote the exposure of both hydrophobic and hydrophilic residues, improving their interaction with water and further aiding solubilization.[51]

When comparing both technologies, the ultrasound (US) treatment produced a slightly higher solubility (99.6%) than hydrodynamic cavitation (98.8%) at 30 min, as determined by both the gravimetric and Bradford assays. This indicates that ultrasound causes more rapid unfolding and disintegration due to the intense localized cavitation energy, whereas prolonged HC exposure leads to gradual and deeper unfolding of protein structures, exposing additional hydrophilic residues and

increasing the protein's affinity for water, thereby enhancing solubility.

In summary, the gravimetric method reflected overall solid dispersion, while the Bradford assay confirmed that the solubility improvement was protein-specific. Both ultrasound and hydrodynamic cavitation significantly enhanced solubility, with ultrasound showing slightly superior efficiency due to its higher cavitational intensity and energy transfer capability.[58]

### 3.6. Effect of US & HC on the turbidity in control and physically modified MPCs

$A_{600}$, representing the absorbance at 600 nm wavelength, is a measure of turbidity in the milk protein concentrate, which can be influenced by processing conditions such as ultrasound power and sonication time. As shown in Fig. 2b, the control sample with no ultrasound treatment, showed an $A_{600}$ value of 0.80 ± 0.05. However, with ultrasound treatment in subsequent trials, significant decreases in absorbance were observed. This decrease in absorbance suggests a reduction in turbidity, indicating the disruption of protein aggregates or particles in the milk protein concentrate as a result of sonication.[59] For T4 (30 min), the lowest $A_{600}$ value of 0.46 ± 0.01 was achieved, indicating the maximum disruptive effects of ultrasound treatment on protein aggregates or particles. The decrease in absorbance observed across the trials reflects the disruption of protein aggregates or particles in the milk protein concentrate. Longer sonication times lead to more effective breakdown of larger protein structures, resulting in a less turbid solution with lower absorbance values.[60] This phenomenon underscores the impact of ultrasound treatment on the physical characteristics of the

protein solution, highlighting its potential for reducing turbidity and improving clarity in various applications, including food processing and beverage production.

For HC treatment, as seen in Fig. 2b, the control sample subjected to no pressure and 0 min of treatment, exhibits an $A_{600}$ value of $0.80 \pm 0.05$, indicating its initial turbidity level. However, with HC treatment in subsequent trials, significant decreases in absorbance were observed, which were statistically different from the control ($p < 0.05$). Similar results were noted in the research done by Hou *et al.*, where hydrodynamic cavitation led to a decrease in aggregation of soybean glycinin (lower turbidity and particle size) under treated conditions as compared to control.[51] The lowest $A_{600}$ value of $0.40 \pm 0.02$ was achieved at 30 min of treatment. The observed decrease in $A_{600}$ values from T1 (5 min) to T4 (30 min) reflects the progressive disruption of larger particles or aggregates into smaller particles or individual molecules due to the influence of HC.[51] This breakdown of particles reduces light scattering and, consequently, turbidity. The effect of HC on turbidity can be attributed to the shear forces and turbulence generated during sonication, which lead to the disintegration of larger protein aggregates and the dispersion of protein particles in the solution.[51] Additionally, prolonged sonication times allow for more extensive disruption of particles, resulting in a greater decrease in turbidity as displayed in Fig. 2b. Therefore, the data indicate that HC has a significant impact on the turbidity of milk protein concentrate, with longer sonication times leading to lower turbidity values, reflecting improved dispersion and homogeneity of the solution. Both HC and US improved the clarity of MPCs by reducing turbidity through the disruption of protein aggregates. However, HC achieved a slightly greater reduction in turbidity with prolonged treatment as compared to US.

### 3.7. Effect of US & HC on the pH in control and physically modified MPCs

pH, which represents the acidity or alkalinity of the solution, is a critical parameter influenced by processing conditions such as ultrasound power and sonication time. As seen in Fig. 3, with 5 min of sonication at 600 W, the pH remains relatively the same, which is statistically similar to the control ($p > 0.05$). This minor variation suggests that short-duration ultrasound treatment does not induce significant changes in pH compared to the control. As sonication time increased in subsequent trials (T2, T3, and T4), slight decreases in pH were observed, which were similar to a previous study conducted by Asaithambi *et al.*, who demonstrated that hydrodynamic cavitation (HC) caused significant structural disruption of egg-white proteins, resulting in a 43% increase in solubility, a reduction in the particle size from 528 nm to 212 nm, and a decrease in surface hydrophobicity by 18%, compared to ultrasound treatment. FTIR analysis further revealed the decrease of α-helix content (from 36% to 28%) and an increase in random coil structures, indicating protein unfolding and exposure of internal residues. These molecular changes collectively enhanced emulsifying and foaming properties, highlighting HC as more effective than ultrasound in improving protein functionality.[23] This decrease
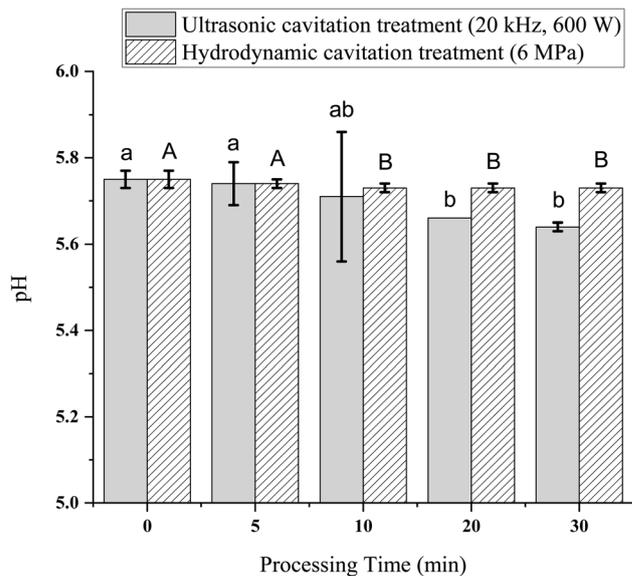


Fig. 3 pH evaluation of 10% w/v MPC modified using ultrasonic cavitation and hydrodynamic cavitation treatments for various time intervals (5, 10, 20, and 30 min) compared to the control sample (untreated). Different lowercase letters at the top of the bars indicate significant differences ($p < 0.05$) in each bar among samples treated at different times.

can be attributed to the prolonged exposure to ultrasound, which induces acoustic cavitation involving the formation and collapse of microscopic bubbles. After 30 min of treatment, the pH decreased to $5.64 \pm 0.01$, the lowest pH observed among all trials. The chemical reactions triggered by cavitation may also lead to the formation of new species impacting the pH. Furthermore, the mechanical stress induced by ultrasound on proteins can cause denaturation, altering the ionization state of amino acid residues and thereby influencing the solution's pH. Additionally, the release of gases or volatile compounds and localized heating during cavitation may contribute to subtle changes in the sample's pH.[61]

With HC treatment, minimal variations in pH are observed (Fig. 3). At 5, 10, 20 and 30 min of treatment, the pH remains relatively stable with no statistically significant difference compared to the control ($p > 0.05$). This consistency in pH across different processing times indicates that HC primarily affects the physical properties of proteins, such as particle size, solubility, and structural integrity, rather than their chemical composition, including pH.[40] Additionally, the pH of the milk protein concentrate may be buffered by other components present in the system, such as salts or buffers, which help maintain pH. It is essential to note that the pH of a solution can influence protein stability and functionality, and while HC may not directly impact pH in this case, it can still affect protein properties through other mechanisms. Therefore, pH remains relatively constant under the tested conditions as displayed in Fig. 3. The inter-treatment comparison shows a divergent trend on the pH of MPCs as US leads to relatively modest decrease in pH of the solution with prolonged exposure, possibly due to protein denaturation and secondary chemical modifications

induced by cavitation. HC however, preserves the original pH, indicating a physical, more mechanical mode of action.

### 3.8. Effect of US & HC on the secondary structures in control and physically modified MPCs

In the context of Fourier-transform infrared (FTIR) spectroscopy, the observation of diminished or broadened peaks in the amide region (approximately 1400–1650 cm$^{-1}$) can often be attributed to the presence of high-water content in the sample solution.[62] Water molecules exhibit strong absorption bands in the same spectral region, thereby obscuring the characteristic amide bands of proteins, which we can observe in Fig. 4a. This interference is particularly pronounced when working with dilute protein solutions, as indicated by the use of the 10% protein concentration in this case. Fig. 4a illustrates the representative FTIR spectrum highlighting the amide A and amide I bands that reflect hydrogen bonding and secondary structure features, respectively. The present study interprets relative transmittance and band shifts qualitatively to compare structural alterations among treatments. Quantitative deconvolution for secondary-structure fractions will be pursued in future work to provide a more detailed insight into conformational transitions induced by US and HC.

To mitigate the challenge posed by high water content in the protein solutions and achieve sharper peaks in the amide region of the FTIR spectra, a strategic approach was employed. Specifically, the samples were subjected to a meticulous drying process by placing them in an oven set at a controlled temperature of 50 °C for an extended duration of 24 h with some modifications. This deliberate desiccation procedure effectively removed excess water molecules from the sample matrices, thereby reducing the interference from water-related spectral contributions. As a result, the FTIR spectra exhibited significantly improved resolution and peak sharpness within the amide region (1400–1650 cm$^{-1}$) (Fig. 4b), allowing for more accurate and precise characterization of the protein's secondary structure and conformation.[63]

Following the meticulous drying process, the FTIR analysis revealed the emergence of distinct and well-defined peaks within the protein region, as illustrated in Fig. 4b. FTIR spectra were processed using OriginPro 2023 for baseline correction, smoothing, and background subtraction to ensure clarity. The analysis focuses on the amide I (1600–1700 cm$^{-1}$) and amide II (1500–1600 cm$^{-1}$) regions to qualitatively assess secondary-structure changes (α-helix, β-sheet, and random coil). Fourier self-deconvolution and curve-fitting were done to provide detailed quantification of structural changes, as shown in Fig. 5a and b. The amide I (1600–1700 cm$^{-1}$) and amide II (1500–1600 cm$^{-1}$) regions were carefully examined to qualitatively assess protein secondary structures. Shifts in the peak position and variations in transmittance intensity were interpreted as indicative of conformational changes in the protein secondary structure (alterations in α-helix, β-sheet, and random coil content). This qualitative approach allowed for comparative evaluation of structural modifications among different milk protein concentrate samples. These observed peaks correspond
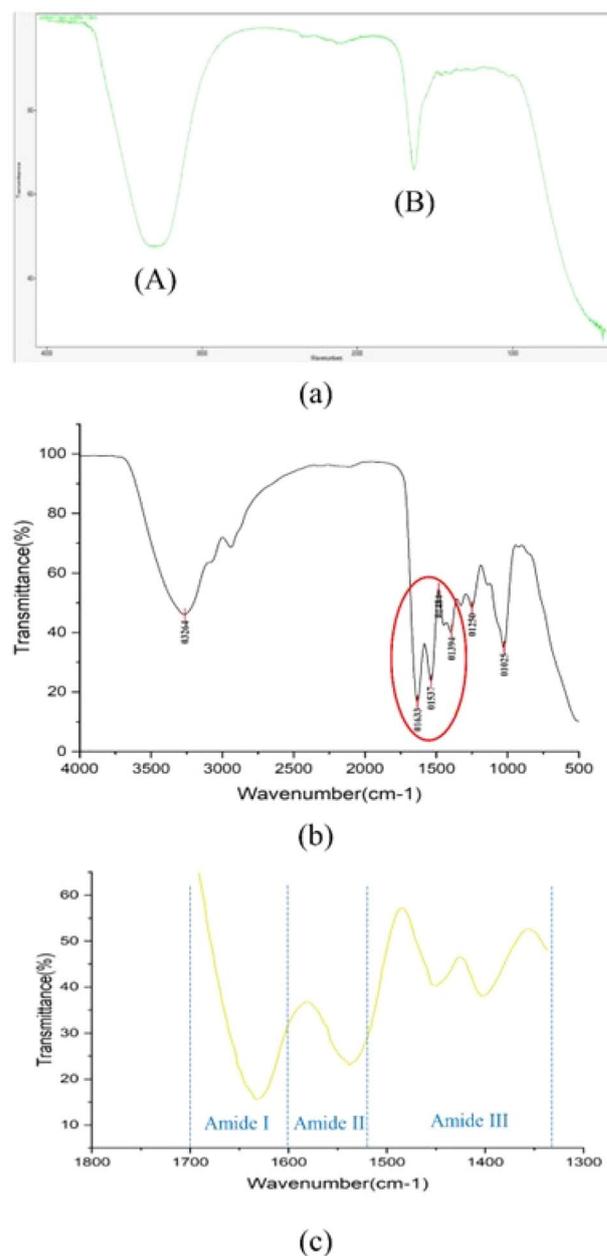


Fig. 4 FTIR spectra of (a) 10% w/v MPC in Mili-Q water without modification (where region 'A' represents the peak for the O–H bond and region 'B' represents the peaks for C–N, N–H, and C=O bonds), (b) 10% w/v MPC without modification dried in a hot air oven at 50 °C for 24 h (where the circle represents the amide regions in the spectrum), (c) 10% w/v MPC without modification enlarged to depict amide I, II, and III regions of the spectrum ranging from wavenumber 1350 to 1650 cm$^{-1}$.

to characteristic amide bands, including amide I at approximately 1633 cm$^{-1}$, amide II at around 1567 cm$^{-1}$, and amide III at approximately 1430 cm$^{-1}$. The presence of these sharp and discernible spectral features signifies the successful removal of excess water content from the samples and the subsequent enhancement of spectral resolution. The precise positions of these peaks as indicated in Fig. 4c provide valuable information about the protein's structural characteristics, including its
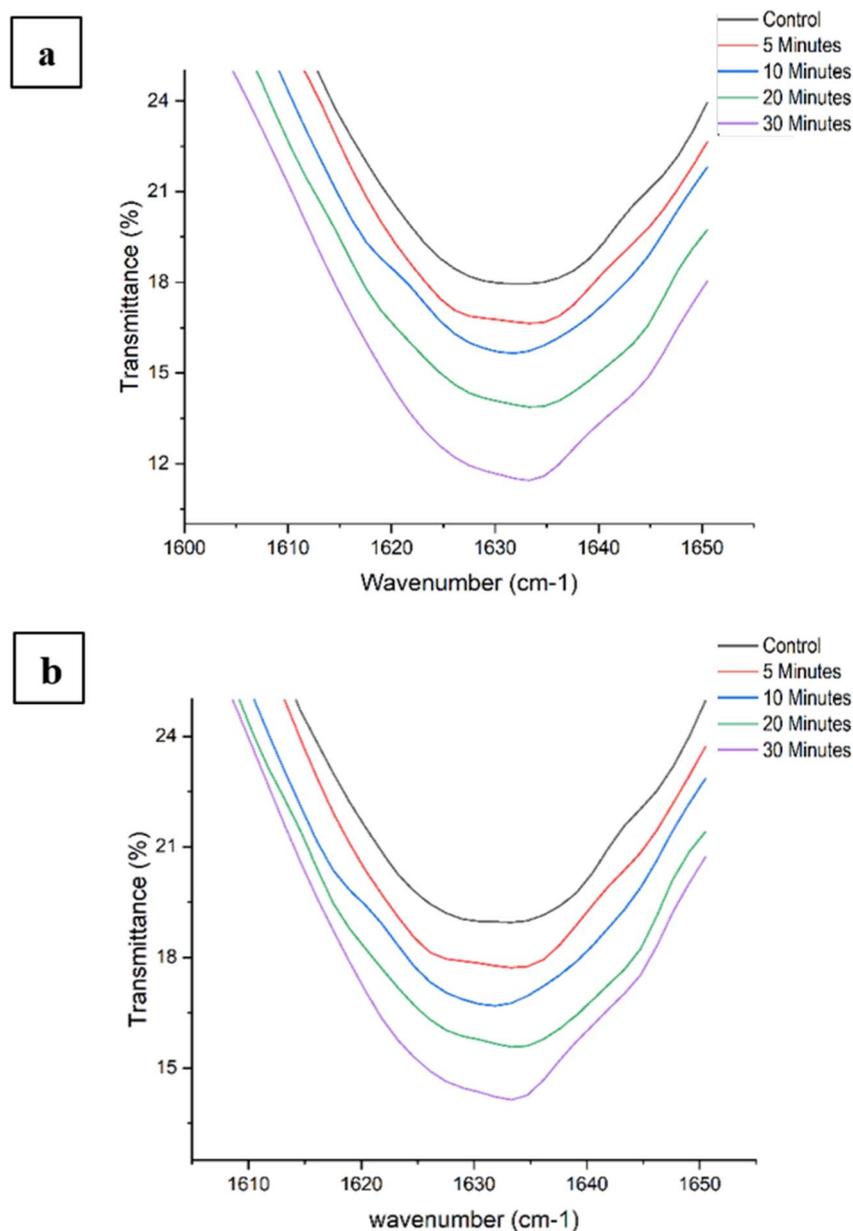
**Fig. 5** FT-IR self-deconvoluted spectra enlarged in the part of the amide I region (wavenumber ranging from 1615 to 1645 cm$^{-1}$) of 10% w/v MPC treated under varying times (0 (control), 5, 10, 20, and 30 min) using (a) ultrasonic cavitation treatment and (b) hydrodynamic cavitation treatment.

secondary structure elements, and serve as a solid foundation for further protein characterization and analysis.

Indeed, the amide I region in FTIR spectra holds a pivotal role in elucidating the secondary structures of proteins.[64] The observed sharp peak in this region at approximately 1633 cm$^{-1}$ reflects the intricate interplay of various structural elements within the protein. The amide I band arises from the stretching vibrations of the C=O bonds, and it is sensitive to the hydrogen bonding patterns and local environments of the peptide backbone. This region provides critical insights into the protein's secondary structure, including the presence and distribution of α-helices, β-sheets, unordered turns, and antiparallel strands.[65] The spectral features within the amide I region are attributed to

the vibrational modes associated with the C=O stretching, N–H in-phase bending, and C–N stretching bonds. The positions and intensities of these peaks can be deconvoluted and analyzed to deduce the specific secondary structure content in the protein, which can be seen in Fig. 4a.

The FTIR spectroscopic analysis reveals distinctive modifications in the secondary structures of the proteins compared to the control sample. In the control, a well-defined peak at 1634 cm$^{-1}$ with a transmittance of 18.12% signifies an organized secondary structure. Conversely, treated samples (T1, T2, T3, and T4) exhibit a notable decrease in the transmittance trend, which was similar to the research done by Mukherjee *et al.,* who investigated the hydration-dependent structural transitions in helical peptides

© 2026 The Author(s). Published by the Royal Society of Chemistry

using FTIR spectroscopy and demonstrated that shifts in the amide I band (primarily 1600–1700 cm$^{-1}$) reflect alterations in the secondary structure. These spectral changes correspond to the unfolding or rearrangement of protein conformation resulting from modified hydrogen-bonding interactions under different hydration states.[65] Fig. 5a presents the FT-IR self-deconvoluted spectra of the enlarged amide I region (1615–1645 cm$^{-1}$) for 10% (w/v) MPC samples subjected to ultrasonic cavitation treatment for different durations (0 min (control), 5, 10, 20, and 30 min). For T1, a peak shift at 1631 cm$^{-1}$ along with a slight decrease in transmittance to 17.51% was observed, suggesting minor structural alterations. T2 displays a broader peak at 1634 cm$^{-1}$ with a diminished transmittance of 15.9%, suggesting increased structural complexity. T3 shows a pronounced broadening at 1628 cm$^{-1}$ with a transmittance of 13.6%, signifying substantial changes in the secondary structure (Fig. 5a).

T4 also exhibits modifications, presenting a peak at 1632 cm$^{-1}$ and transmittance of 11.2%, reflecting further structural evolution. This could be because the energy input from cavitation can cause alpha-helices to unravel into random coils, reducing the number of ordered structures. This transition is often detectable by changes in the amide I and amide II bands in the FTIR spectrum, and the disruption of secondary structures can promote the formation of beta-sheet aggregates, particularly in proteins prone to amyloid formation. This aggregation can manifest as new absorption bands or shifts in existing ones. These alterations in the peak position and transmittance across the treated samples suggest a progressive disruption in the native secondary structure of the proteins as ultrasonication treatment intensifies.[66] The observed shifts and broadening in the amide I band indicate potential variations in alpha-helix, beta-sheet, or random coil structures. The decreasing transmittance values further underscore the evolving conformational changes induced by ultrasonication.

As illustrated in Fig. 5b, for HC treatment, the amide I region in the FTIR self-deconvoluted spectrum plays a crucial role in revealing the secondary structural characteristics of proteins.[52] The observed sharp peak in this region at approximately 1633 cm$^{-1}$ reflects the intricate interplay of various structural elements within the protein. The amide I band arises from the stretching vibrations of the C=O bonds, and it is sensitive to the hydrogen bonding patterns and local environments of the peptide backbone.[65] The spectral features within the amide I region are attributed to the vibrational modes associated with the C=O stretching, N–H in-phase bending, and C–N stretching bonds. The positions and intensities of these peaks can be deconvoluted and analyzed to deduce the specific secondary structure content in the protein.[65]

The FTIR spectroscopic analysis reveals distinctive modifications in the secondary structure of the proteins compared to the control sample. For the control sample, a well-defined peak at 1634 cm$^{-1}$ with a transmittance of 18.12% signifies an organized secondary structure that is similar to the research done by Xu & Zhang et al.[67] Conversely, treated samples (T1, T2, T3, and T4) exhibit a notable decrease in the transmittance trend. T1 demonstrates a peak shift at 1631 cm$^{-1}$ and a slightly reduced transmittance of 17.95%, indicating subtle structural

modifications. T2 displays a broader peak at 1634 cm$^{-1}$ with a diminished transmittance of 16.5%, suggesting decreased structural complexity. T3 shows pronounced broadening at 1628 cm$^{-1}$ with a transmittance of 15.6%, signifying substantial changes in the secondary structure. T4 also exhibits modifications, presenting a peak at 1632 cm$^{-1}$ and a transmittance of 13.8%, reflecting further structural evolution. This could be because the energy input from cavitation can cause alpha-helices to unravel into random coils, reducing the number of ordered structures.

This transition is often detectable by changes in the amide I and amide II bands in the FTIR spectrum and also the disruption of secondary structures can promote the formation of beta-sheet aggregates, particularly in proteins prone to amyloid formation.[65] This aggregation can manifest as new absorption bands or shifts in existing ones. These alterations in the peak position and transmittance across the treated samples suggest a progressive disruption in the native secondary structure of the proteins as HC treatment intensifies where shear forces can unfold proteins mechanically, exposing internal residues to the surrounding environment, which alters the FTIR absorption profile.[23] While both HC and US significantly impact the secondary structure of MPCs, US (11.2% transmittance) leads to more aggressive unfolding and extensive denaturation with prolonged exposure as compared to HC (13.8%). This unfolding can help in improving the functional characteristics of proteins such as solubility and increased digestibility. These functional improvements expand the potential for US and HC-processed MPCs in a wide range of food applications.[20]

### 3.9. Effect of US & HC on the primary structure in control and physically modified MPCs

The SDS-PAGE patterns of treated and untreated MPC samples are shown in Fig. 6a and b. In lane 1, a protein ladder serves a reference for molecular weight determination. Lane 2 featuring the test protein, showcases bands corresponding to lactoferrin (approximately 80 kDa) and serum albumin (around 70 kDa). Lanes 1 and 3 represent untreated milk protein, whereas lane 2 represents test protein, and lanes 4, 5, 6, and 7 represent milk protein treated with ultrasound for 5, 10, 20, and 30 min. Notably, the SDS-PAGE profiles across these lanes exhibit consistent bands for lactoferrin, serum albumin, and casein proteins (including αS2-CN, αS1-CN, β-CN, and k-CN) in the molecular weight range of 15 to 20 kDa. The absence of discernible shifts in molecular weights between untreated and treated samples suggests that the ultrasound treatment employed in this study does not induce significant modifications in the molecular weights of milk proteins, similar to the research done by O'Sullivan et al.[68] This is because peptide bonds are highly stable covalent bonds, requiring substantial energy to break. The US power might not reach the threshold needed to cleave these bonds, leaving the primary structure intact, and cavitation effectively disrupts hydrogen bonds and other non-covalent interactions stabilizing the secondary and tertiary structures.[22]

Concerning HC, the absence of discernible shifts in molecular weights between untreated and treated samples suggests
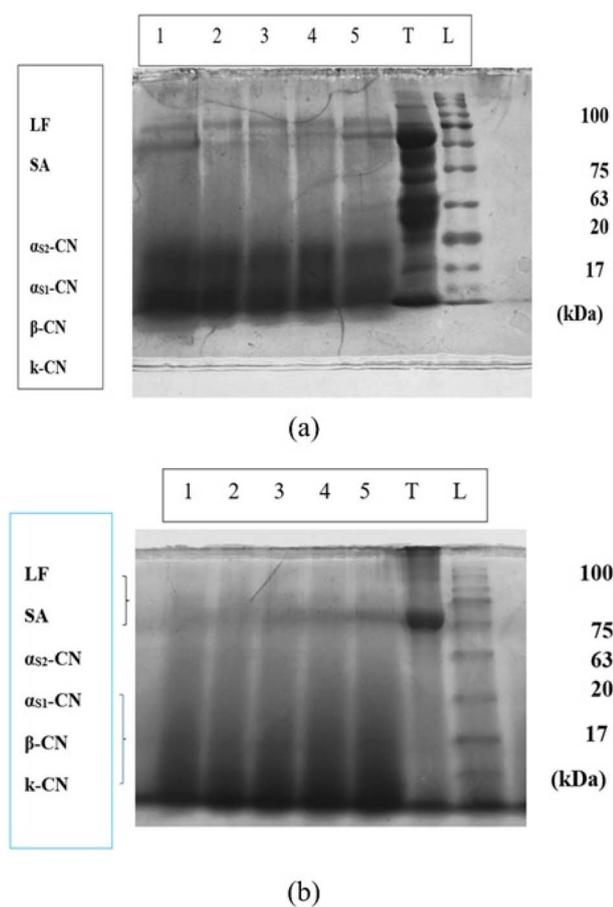
**Fig. 6** SDS-PAGE pattern for 100 mL of 10% w/v MPC corresponding to (a) untreated and ultrasonic cavitation treatment and (b) untreated and hydrodynamic cavitation treatment (where L: protein ladder; T: test protein; 1: untreated; 2, 3, 4, and 5: treated for 5, 10, 20, and 30 min, respectively; LF: lactoferrin; SA: serum albumin).

that the HC treatment employed in this study does not induce significant modifications in the molecular weights of milk proteins, which is similar to the research done by Ren *et al.*[69] Similar to US-treated samples, the distinct bands representing lactoferrin, serum albumin, and casein proteins remain unaltered. This could be because the cavitation power may be strong enough to induce some structural stress and minor conformational changes but not enough to break peptide bonds. This subthreshold energy input is sufficient to alter the protein's secondary and tertiary structures without affecting the primary structure, and the transient nature of cavitation bubbles and the rapid pressure changes cause alterations in higher-order structures, leaving the covalent backbone of the protein unchanged.[57] Furthermore, the stability of these proteins against HC suggests their potential suitability for various industrial applications where protein integrity is paramount.

## 4 Conclusion

In conclusion, the optimization of both US and HC techniques for milk protein modification has yielded significant improvements in emulsifying and foaming properties. The study focused on enhancing MPCs using advanced US and HC techniques to improve its properties for food applications. Use of these easy-to-scale, novel technologies resulted in significant improvements across various functional properties of MPCs, such as emulsifying, foaming, solubility, and turbidity along with modifications in primary as well as secondary structures of MPCs. When compared to US cavitation, HC-treated samples achieved more pronounced results for emulsifying and foaming properties. Throughout the research, pH levels remained stable, showing minimal changes, indicating good product stability with US and hydrodynamic cavitation. This is particularly important for applications in products where pH sensitivity could affect the product's shelf life. The structural modifications in MPCs were identified using FTIR spectroscopy, which indicated shifts in the secondary structure due to cavitation. However, SDS-PAGE analysis confirmed that the absence of new low-molecular-weight bands indicated that cavitation did not cleave peptide bonds or alter molecular integrity. These findings offer valuable insights for tailoring physical treatments such as US and HC for improving functional requirements for suitable industrial applications.

## Author contributions

Shreyas H. K.: data curation, investigation, methodology, software, validation, writing – original draft, Preeti Adhikari: writing – review & editing, data curation. Anas Ejaz Yasmeen Shaikh: writing – review and editing. Shalini S. Arya: conceptualization, data curation, investigation, project administration, resources, supervision, validation, visualization, writing – review and editing.

## Conflicts of interest

The authors declare no conflicts of interest.

## Data availability

The data supporting this article have been included as part of the Supplementary Information (SI). Supplementary information: effect of HC and US on physical properties of MPC. Fig. S1–S8, Tables S1 and S2. See DOI: https://doi.org/10.1039/d5fb00393h.

## Acknowledgements

## References

1 M. Iddir, A. Brito, G. Dingeo, S. S. Fernandez Del Campo, H. Samouda, M. R. La Frano and T. Bohn, *Nutrients*, 2020, **12**(6), 1562, DOI: 10.3390/nu12061562.

2 L. Sha and Y. L. Xiong, *Trends Food Sci. Technol.*, 2020, **102**, 51–61.

3 J. Małecki, S. Muszyński and B. G. Sołowiej, *Polymers*, 2021, **13**, 2506, DOI: 10.3390/polym13152506.

4 Y. Dai, G. X. Cai, Y. Liang, Z. Y. He, Y. Zhang, C. H. Li and H. J. Chang, *Int. J. Food Prop.*, 2024, **27**, 870–882.

5 Z. Zheng, L. Zhang, M. Zhang, A. S. Mujumdar and Y. Liu, *Food Chem.*, 2023, **417**, 135769, DOI: 10.1016/j.foodchem.2023.135769.

6 H. Lesme, C. Rannou, M. H. Famelart, S. Bouhallab and C. Prost, *Trends Food Sci. Technol.*, 2020, **98**, 140–149.

7 M. Messina and V. Messina, *Front. Plant Sci.*, 2024, **15**, DOI: 10.3389/fpls.2024.1407506.

8 W. F. Elkot, A. Elmahdy, H. Talaat, O. A. Alghamdia, S. K. Alhag, E. A. Al-Shahari and H. A. Ismail, *Int. J. Biol. Macromol.*, 2024, **258**, 128999, DOI: 10.1016/j.ijbiomac.2023.128999.

9 M. Tarahi, L. Abdolalizadeh and S. Hedayati, *Food Chem.*, 2024, **444**, 138626, DOI: 10.1016/j.foodchem.2024.138626.

10 R. Gundogan, G. S. Tomar, A. C. Karaca, E. Capanoglu and M. C. Tulbek, *Sustainable Protein Sources*, 2024, 185–199, DOI: 10.1016/B978-0-323-91652-3.00007-1.

11 W. Zeng, J. Xue, H. Geng, X. Liu, J. Yang, W. Shen and Q. Zhu, *Biotechnol. Bioeng.*, 2024, **121**, 799–822.

12 M. T. Reetz, G. Qu and Z. Sun, *Nat. Synth.*, 2024, **3**, 19–32.

13 J. C. Banach, Z. Lin and B. P. Lamsal, *LWT Food Sci. Technol.*, 2013, **54**, 397–403.

14 G. Ryan, A. B. Nongonierma, J. O'Regan and R. J. FitzGerald, *Int. Dairy J.*, 2018, **81**, 113–121.

15 L. Cadesky, M. Walkling-Ribeiro, K. T. Kriner, M. V. Karwe and C. I. Moraru, *J. Dairy Sci.*, 2017, **100**, 7055–7070.

16 D. Liu, in *Handbook of Molecular Biotechnology*, ed. D. Liu, CRC Press, Boca Raton, 1st edn, 2024, pp. 285–292.

17 E. Bormashenko, Y. Bormashenko, I. Legchenkova and N. M. Eren, *Innovative Food Sci. Emerg. Technol.*, 2021, **72**, 102759, DOI: 10.1016/j.ifset.2021.102759.

18 Q. Sui, H. Roginski, R. P. Williams, C. Versteeg and J. Wan, *Int. Dairy J.*, 2011, **21**, 206–213.

19 J. Pan, Z. Zhang, B. K. Mintah, H. Xu, M. Dabbour, Y. Cheng, C. Dai, R. He and H. Ma, *J. Food Process Eng.*, 2022, **45**(4), DOI: 10.1111/jfpe.14010.

20 M. A. Malik, H. K. Sharma and C. S. Saini, *Ultrason. Sonochem.*, 2017, **39**, 511–519.

21 B. Wang, H. Su and B. Zhang, *Chem. Eng. J.*, 2021, **412**, 128685, DOI: 10.1016/j.cej.2021.128685.

22 C. Li, F. Yang, Y. Huang, C. Huang, K. Zhang and L. Yan, *J. Food Eng.*, 2020, **265**, 109697, DOI: 10.1016/j.jfoodeng.2019.109697.

23 N. Asaithambi, P. Singha and S. K. Singh, *Innovative Food Sci. Emerg. Technol.*, 2022, **82**, 103166, DOI: 10.1016/j.ifset.2022.103166.

24 C. Patil, S. Sonawane, P. Bhalerao and A. Dabade, *J. Agric. Food Res.*, 2023, **14**, 100899, DOI: 10.1016/j.jafr.2023.100899.

25 A. R. Salve, K. Pegu and S. S. Arya, *Ultrason. Sonochem.*, 2019, **59**, 104728, DOI: 10.1016/j.ultsonch.2019.104728.

26 B. Ilirjana and G. Bardhi, *Conference: RENS*, 2013.

27 A. Jokar and M. H. Azizi, *Food Sci. Nutr.*, 2022, **10**, 1126–1134, DOI: 10.1002/fsn3.2772.

28 K. Pegu, P. More and S. S. Arya, *Food Bioprod. Process.*, 2023, **141**, 49–59, DOI: 10.1016/j.fbp.2023.07.003.

29 P. Voudouris, H. C. Mocking-Bode, L. M. Sagis, C. V. Nikiforidis, M. B. Meinders and J. Yang, *Food Hydrocolloids*, 2025, **160**, 110754, DOI: 10.1016/j.foodhyd.2024.110754.

30 D. Xu, F. Yuan, J. Jiang, X. Wang, Z. Hou and Y. Gao, *Innovative Food Sci. Emerg. Technol.*, 2011, **12**, 32–37, DOI: 10.1016/j.ifset.2010.10.001P.

31 S. Kalkan, M. R. Otağ and M. S. Engin, *Food Chem.*, 2020, **307**, 125524, DOI: 10.1016/j.foodchem.2019.125524.

32 A. Minorova, I. Romanchuk, Y. Zhukova, N. Krushelnytska and S. Vezhlivtseva, *Agric. Sci. Pract.*, 2017, **4**, 52–58, DOI: 10.15407/agrisp4.02.052.

33 L. S. Rupp, M. S. Molitor and J. A. Lucey, *J. Dairy Sci.*, 2018, **101**, 7702–7713, DOI: 10.3168/jds.2018-14383.

34 Y. Sun, X. Yu, M. Hussain, X. Li, L. Liu, Y. Liu, S. Ma, K. Kouame, C. Li, Y. Leng and S. Jiang, *Ultrason. Sonochem.*, 2022, **82**, 105881, DOI: 10.1016/j.ultsonch.2021.105881.

35 H. Uluko, L. Liu, J. P. Lv and S. W. Zhang, *Crit. Rev. Food Sci. Nutr.*, 2016, **56**, 1193–1208, DOI: 10.1080/10408398.2012.758625.

36 Y. Zhang, Z. Qian, B. Ji and Y. Wu, *Renewable Sustainable Energy Rev.*, 2016, **56**, 303–318.

37 S. Shokri, F. Javanmardi, M. Mohammadi and A. M. Khaneghah, *Ultrason. Sonochem.*, 2022, **83**, 105938, DOI: 10.1016/j.ultsonch.2022.105938.

38 C. Li, X. Rui, Y. Zhang, F. Cai, X. Chen and M. Jiang, *LWT–Food Sci. Technol.*, 2017, **82**, 227–234, DOI: 10.1016/j.lwt.2017.04.054.

39 A. Taha, E. Ahmed, A. Ismaiel, M. Ashokkumar, X. Xu, S. Pan and H. Hu, *Trends Food Sci. Technol.*, 2020, **105**, 363–377.

40 A. R. Jambrak, T. J. Mason, V. Lelas, Z. Herceg and I. L. Herceg, *J. Food Eng.*, 2008, **86**, 281–287.

41 J. J. O'Sullivan, C. J. Espinoza, O. Mihailova and F. Alberini, *Ultrason. Sonochem.*, 2018, **48**, 218–230.

42 A. Chávez-Martínez, R. Reyes-Villagrana, A. L. Rentería-Monterrubio, R. Sánchez-Vega, J. M. Tirado-Gallegos and N. A. Bolivar-Jacobo, *Foods*, 2020, **9**, 1688, DOI: 10.3390/foods9111688.

43 A. D. Alarcon-Rojo, L. M. Carrillo-Lopez, R. Reyes-Villagrana, M. Huerta-Jiménez and I. A. Garcia-Galicia, *Ultrason. Sonochem.*, 2019, **55**, 369–382.

44 S. Nazari, S. Z. Shafaei, A. Hassanzadeh, A. Azizi, M. Gharabaghi, R. Ahmadi and B. Shahbazi, *Physicochem. Probl. Miner. Process.*, 2020, **56**, 884–904, DOI: 10.37190/ppmp/126628.

45 N. Asaithambi, P. Singha, M. Dwivedi and S. K. Singh, *J. Food Process Eng.*, 2019, **42**, e13144, DOI: 10.1111/jfpe.13144.

46 A. Mimouni, H. C. Deeth, A. K. Whittaker, M. J. Gidley and B. R. Bhandari, *Food hydrocolloids*, 2009, **23**, 1958–1965.

47 D. Nagy, M. A. Lambertné, T. Zsom and M. V. Zsomné, *Animal Welfare, Ethology and Housing Systems*, 2018, **14**, 45–52.

48 C. Anandharamakrishnan, in *Handbook of Drying for Dairy*, 2017, pp. 1–14.

49 Y. Hou, X. E. Ren, Y. Huang, K. Xie, K. Wang, L. Wang and F. Yang, *Front. Nutr.*, 2023, **10**, 113615, DOI: 10.1016/j.lwt.2022.113615.

50 J. V. Silva and J. A. O'Mahony, Flowability and wetting behavior of milk protein ingredients as influenced by powder composition, particle size and microstructure, *Int. J. Dairy Technol.*, 2017, **70**(2), 277–286, DOI: 10.1111/1471-0307.12368.

51 Y. Hou, F. Yang, J. Cao, Y. Huang, C. Li and J. Li, *LWT*, 2022, **163**, 113615, DOI: 10.1016/j.lwt.2022.113615.

52 S. Kakade, S. Sonawane, P. Bhalerao and A. Dabade, *Meas.: Food*, 2024, **14**, 100164, DOI: 10.1016/j.meafoo.2024.100164.

53 C. Puppo, N. Chapleau, F. Speroni, M. de Lamballerie-Anton, F. Michel, C. Añón and M. Anton, *J. Agric. Food Chem.*, 2004, **52**, 1564–1571.

54 R. Morales, K. D. Martínez, V. M. P. Ruiz-Henestrosa and A. M. Pilosof, *Ultrason. Sonochem.*, 2015, **26**, 48–55.

55 A. R. Jambrak, T. J. Mason, V. Lelas, L. Paniwnyk and Z. Herceg, *J. Food Eng.*, 2014, **121**, 15–23.

56 P. R. Gogate and A. B. Pandit, *Ultrason. Sonochem.*, 2005, **12**, 21–27.

57 H. Kamal, A. Ali, S. Manickam and C. F. Le, *Food Chem.*, 2023, **407**, 135071, DOI: 10.1016/j.foodchem.2022.135071.

58 G. Yildiz, J. Andrade, N. E. Engeseth and H. Feng, *J. Colloid Interface Sci.*, 2017, **505**, 836–846.

59 M. H. Omura, A. P. H. de Oliveira, L. de Souza Soares, J. S. dos Reis Coimbra, F. A. R. de Barros, M. C. T. R. Vidigal and E. B. de Oliveira, *Food Hydrocolloids*, 2021, **113**, 106457, DOI: 10.1016/j.foodhyd.2020.106457.

60 S. M. T. Gharibzahedi and B. Smith, *Trends Food Sci. Technol.*, 2020, **98**, 107–116.

61 A. Amiri, P. Sharifian and N. Soltanizadeh, *Int. J. Biol. Macromol.*, 2018, **111**, 139–147.

62 H. Yang, S. Yang, J. Kong, A. Dong and S. Yu, *Nat. Protoc.*, 2015, **10**, 382–396.

63 S. Magalhães, B. J. Goodfellow and A. Nunes, *Appl. Spectrosc. Rev.*, 2021, **56**, 869–907.

64 S. Cai and B. R. Singh, *Biochemistry*, 2004, **43**, 2541–2549.

65 S. Mukherjee, P. Chowdhury and F. Gai, *J. Phys. Chem. B*, 2007, **111**, 4596–4602.

66 U. Roobab, B. R. Chen, G. M. Madni, Z. G. Tong, X. A. Zeng, G. Abdi, S. Hussain and R. M. Aadil, *Ultrason. Sonochem.*, 2024, **107**, 106919, DOI: 10.1016/j.ultsonch.2024.106919.

67 D. Xu and Y. Zhang, *Biophys. J.*, 2011, **101**, 2525–2534.

68 J. O'Sullivan, M. Arellano, R. Pichot and I. Norton, *Food Hydrocolloids*, 2014, **42**, 386–396.

69 Z. Ren, Z. Chen, Y. Zhang, X. Lin and B. Li, *Food Hydrocolloids*, 2019, **96**, 322–330.